

Purification of rare-earth metals as the approach to improving properties of hard magnetic Nd₂Fe₁₄B-based materials

N B Kolchugina^{1,*}, G S. Burkhanov¹, A G Dormidontov², A A Lukin², Yu S Koshkid'ko^{3,4}, K Skotnicová³, H Drulis⁵ and B Smetana³

¹ Baikov Institute of Metallurgy and Materials Science, Russian Academy of Science, Leninskii pr. 49, 119991 Moscow, Russia

² JSC "Spetsmagnit", Dmitrovskoe sh. 58, 127238 Moscow, Russia

³ Vysoka Skola banska - Technical University of Ostrava, 70833, 17 Listopadu, 15/2172, Ostrava-Poruba, Czech Republic

⁴ International Laboratory for High Magnetic Fields and Low Temperatures, Polish Academy of Sciences, Gajowicka 95, 53-421 Wroclaw, Poland

⁵ Institute of Low Temperature and Structure Research, Polish Academy of Sciences, Okolna 2, 50-422 Wroclaw, Poland

*E-mail: natalik014@yandex.ru

Abstract. Purification of rare-earth metals, namely, Nd, Pr, Tb, Dy used in manufacturing Nd₂Fe₁₄B-based magnets was realized. The metals were purified by vacuum distillation/sublimation. Conditions of the process were optimized and the structure of distilled metals was studied. Distilled terbium and dysprosium were used to prepare hydrides TbH₂ and DyH₂. Peculiarities of the decomposition of terbium and dysprosium hydrides were studied with the view of the use of the compounds as efficient additions, which allow the high-coercivity state of sintered magnets to be formed. Terbium hydride additions (to 4 wt %) favor the marked increase in the magnetization coercive force without excessive attenuation of the remanence ($jH_c = 1940$ kA/m, $(BH_{max}) = 292$ kJ/m³). Dysprosium hydride additions increase the stability of high-coercivity state ($jH_c = 1310$ kA/m, $(BH_{max}) = 322$ kJ/m³ at 2 wt% DyH₂).

1. Introduction

Requirements for the purity of metals and substances, as a rule, are determined experimentally and depend on their end use. Rare-earth metals 95-99% purity (with respect to other rare-earth metals) are known to be suitable for manufacturing hard-magnetic, magnetostrictive, and hydrogen-storage materials. For these applications, mixtures of rare-earth metals also can be used. However, in recent years, investigators trend to discuss the properties of permanent magnets in relation to the purity of starting materials and substantial dependence of magnetic characteristics on manufacturing conditions. In accordance with [1], three grades of rare-earth metals (REMs) can be defined; these are (1) ultrapure, (2) routine metals prepared under laboratory conditions, and (3) commercial. The purity of high pure REMs is > 99.0 at % with respect to all elements in the periodic table. The purity of metals prepared under laboratory conditions is 99% with allowance for all elements. The content of base metal in commercial REMs is <98 at %. The transition from the commercial-purity metal to the metal



corresponding to the next purity grade leads to about tenfold increases in the metal cost. The most important application of neodymium is Nd-Fe-B magnets. Sintered Nd-Fe-B magnets find wide applications for technology owing to the high maximum energy product (BH_{\max}), remanence (B_r), and magnetization coercive force (jH_c) [2]. To increase jH_c , which is responsible for the time-temperature stability of sintered magnets, the basic $Nd_{14-15}Fe_{oct}.B_{6-8}$ composition is alloyed with Pr, Dy, Tb (to increase the anisotropy field of the 2-14-1 phase); moreover, the following technological processes are used: “strip-casting”, hydrogen decrepitation, mechanical alloying, diffusion saturation of rare-earth magnet surface with Dy and Tb, and multi-stage heat treatments at 450-1000°C [2-7]. The coercivity of Nd-Fe-B magnets is structure sensitive and dependent on the continuity and composition of REM-rich phases, grain-boundary defects, average grain size, exchange interaction between $Nd_2Fe_{14}B$ hard magnetic grains, etc. The coercivity of sintered magnets is reached by post-sintering annealing at the optimum temperature (around 500°C). The role of the low-temperature heat treatment consists in the formation of continuous non-magnetic REM-rich layers between $(Nd,REM)_2Fe_{14}B$ grains.

The experiments with Dy and Tb additions are carried out to achieve the optimum microstructure, which involves confining the Dy distribution to the grain boundary regions [4,7]. If Dy can be confined in the grain boundary regions, then: (1) it should be possible to increase locally the coercivity and hence reduce the probability of reverse domains forming at the grain boundaries; (2) limit the substitution of Nd by Dy in the matrix phase and thus limit the reduction of the magnetization and hence the remanence; and (3) reduce the amount of Dy required to achieve a particular increase in the coercivity and hence reduce the overall cost of the alloy.

The oxygen content and character of distribution of oxide inclusions are known to determine to a great extent the quality of Nd-Fe-B magnets. Thus, the probability of formation of oxide compounds in the course of production of Nd-Fe-B magnets is sufficiently high.

The alloying of the basic composition with rare-earth metals added in the form of hydrides was performed in [8-12]. According to data of [10], a relatively Dy-rich phase formed in the Nd-rich grain boundary phase and this slowed down the substitution of Dy for Nd in the $Nd_2Fe_{14}B$ -based matrix phase, possibly enhancing local coercivity without excessive attenuation of the remanence. The magnetic and microstructural modification of the Nd-Fe-B sintered magnet by mixed DyF_3/DyH_x powder doping was studied in [11]. The possibility of application of dysprosium hydride nanoparticles for wastes processing is discussed in [12]; in this case, the properties of prepared magnets are: $B_r = 1.296$ T, $jH_c = 1360$ kA/m, $(BH)_{\max} = 292.3$ kJ/m³.

There are a few studies devoted to the investigation of the kinetics of metal hydrides, in particular, rare-earth metal hydrides in the literature [13, 14]. Temperatures of the onset of the hydride decomposition demonstrate variations.

The aim of the present study is to demonstrate the improvement of Nd-Fe-B permanent magnet characteristics by using hydrides of heavy REMs, the purity of which is retained and controlled during hydride synthesis and application as the component of powder mixture. The role of the hydride additions in the formation of magnet characteristics is demonstrated. In the course of the study, we state the efficiency of vacuum distillation for the purification of REMs, which is accompanied by the formation of nontraditional structural morphology of the metals.

2. Experimental Procedure, Results and Discussion

2.1. Purification of REMs

Technology for purification of rare-earth metals by vacuum distillation (Y, Pr, Nd, Gd, Tb, Lu) and sublimation (Sc, Dy, Ho, Er, Tm) and optimum regimes of the purification have been elaborated at the Baikov Institute of Metallurgy and Materials Science [15]. The purification is performed at a residual pressure of 10^{-4} - 10^{-5} Pa in a resistor furnace equipped with a graphite heater. A REM is evaporated from a tantalum crucible and deposited on a water-cooled copper condenser in the form of a druse (150-250 g) of small crystal growing together. Figure 1a shows the appearance of a distilled REM. The structure of distilled REMs was studied in air by atomic force microscopy using a Solver Pro EC (NT MDT) atomic-force microscope and semicontact regime. The studies allow us to conclude the

existence of the unique morphology of distilled metals. Their structures are characterized by structural components differing in the dispersivity: elongated crystals (single crystals) are from 0.5 to 2.5 μm in lateral size and nano-sized grains, which are observed within spaces between elongated crystals and fasten them together. The developed surface of distilled metal is characterized by steps and terraces, which are formed in the course of deposition from vapor. According to atomic-force microscopy (AFM) data, the height of steps is from 15 to 80 nm, which can correspond to a grain size of ~ 30 nm. Figures 1b,c show AFM images of distillate structure (transverse and longitudinal sections), which confirm the existence of nano-sized structure [16].

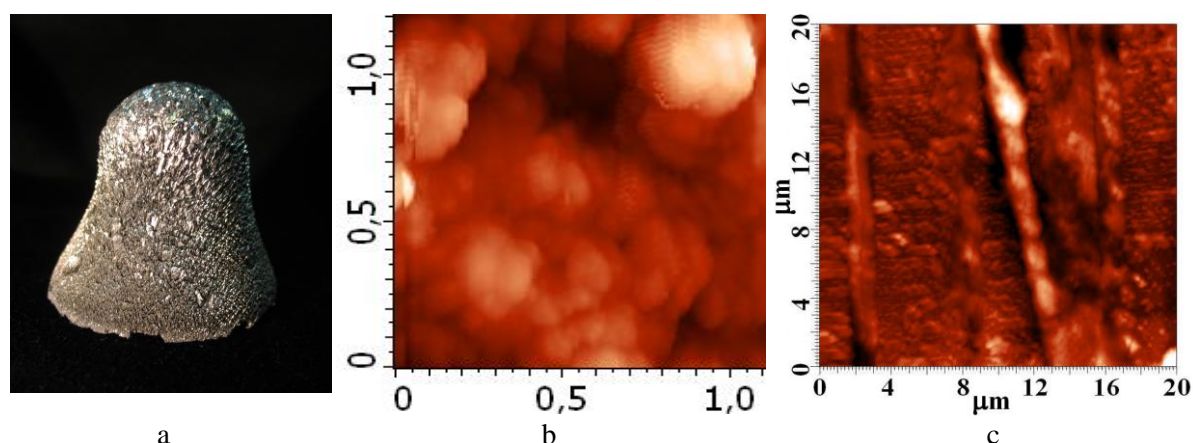


Figure 1. (a) Appearance of distilled REMs and AFM images of the surface of (a) transverse and (b) longitudinal sections of distilled gadolinium.

REMs purified by vacuum distillation/sublimation in accordance with the process are characterized by low contents of (1) gas-forming elements, (2) volatile and refractory elements, (3) other rare-earth metals, and (4) Fe, Cu, Al contents of $\sim 10^{-3}$ wt %. Figures 2a,b shows impurity-distribution histograms for distilled praseodymium, neodymium, and terbium. We can state that distillation process is more efficient for neodymium. The metals can be classified among high-purity REMs.

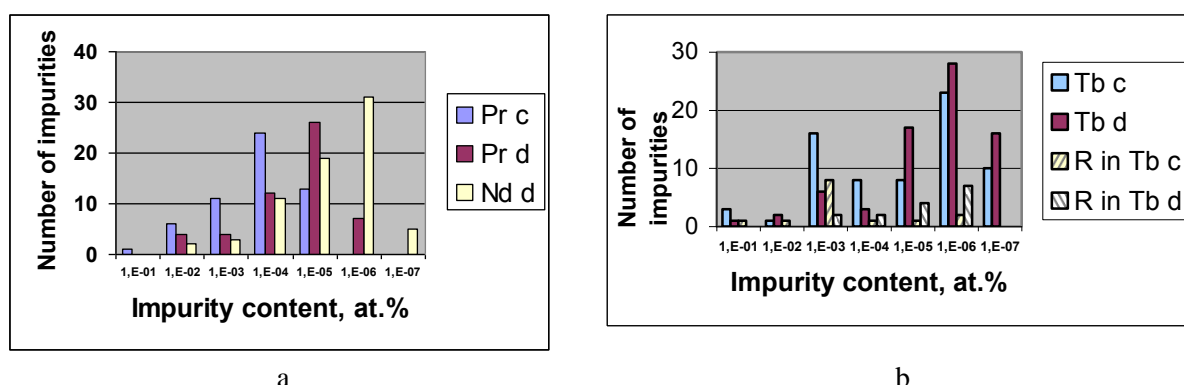


Figure 2. Impurity distribution histograms for (a) Pr commercial (Pr c) and distilled (Pr d) and distilled Nd (Nd d) and (b) Tb commercial (Tb c) and distilled (Tb d); R = REMs.

We have demonstrated the opportunities of distillation technology for the preparation of considerable quantities of high-purity REMs. Thus, the process can be recommended for application in small-capacity works since it realizes the optimum relationship metal purity, its cost, and process efficiency. The purity of REMs can be increased when distillation/sublimation is performed in decreasing the evaporation rate via varying the evaporation temperature.

2.2. Study of REMs hydrides

REM dihydrides samples (TbH_{2} and DyH_{2}) were prepared by direct reaction of gaseous hydrogen with distilled metals using a glass Sieverts-type apparatus. The hydrogenation was carried out using pure hydrogen gas under pressures up to 0.1 MPa obtained from TiH_2 hydrogen storage. The amount of absorbed hydrogen was determined by measurements of hydrogen pressure change in the reactor chamber after finishing the hydrogenation reaction. This allows one to calculate the hydrogen concentration in the sample with an accuracy of ± 0.02 H/f.u. After synthesis, the hydride samples were homogenized (annealed) for 72 h at 350°C . The obtained hydrides were breakable.

Kinetics of molecular hydrogen evolution from the terbium hydride was studied by Dr. V.S. Petrov using a MS-200 standard gas mass-spectrometer equipped with an evaporating attachment to operated in a temperature range of from 20 to 1000°C (the residual pressure in the cold system is $5 \cdot 10^{-5}$ Pa). Weight losses were controlled using a balance. The decomposition of dysprosium was studied by gravimetric analysis. Figure 3a shows data on the kinetics of decomposition of terbium dihydride.

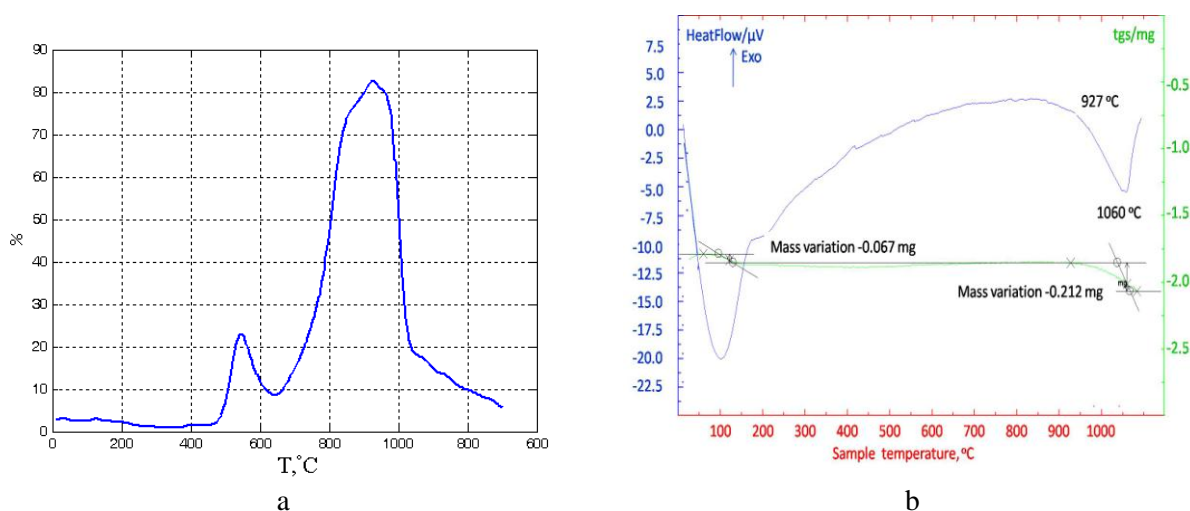


Figure 3. (a) Density of hydrogen desorption flow during TbH_2 decomposition; (b) DTA and TGA curves for DyH_2 dysprosium hydride decomposition.

The studies allowed us to determine the temperatures of the onset of terbium hydride decomposition and temperature range corresponding to intense hydrogen evolution. The hydrogen evolution is characterized by two peaks. The temperatures of the peaks do not correlate with those determined earlier in [14] (the onset, peak and end of decomposition correspond to 620 , 750 , and 800°C , respectively). It is likely that the discrepancies are related to different both purity of initial metals, conditions of sample preparation, composition of hydrides, and hydrogen-evolution recording techniques. In our opinion, the low-temperature peak in the hydrogen desorption flow is related to the surface and near-surface hydrogen evolution as a result of decomposition of terbium trihydride that is present in small amounts. The maximum hydrogen-evolution is reached at $\sim 900^\circ\text{C}$. The decrease in the hydrogen flow at $\sim 650^\circ\text{C}$ is related to the hydrogen depletion of the surface and near-surface layers. We cannot relate specifically each of peaks or each component of high-temperature peaks with decomposition processes (hydride decomposition or hydrogen solid solution decomposition), but we can recommend to hold samples at temperatures above 1000°C for 1 h to ensure the more complete hydrogen evolution. Earlier, we have found that, after the decomposition of terbium dihydride, reduced terbium actively fixes oxygen to form the terbium oxide. Thus, the use of terbium particles or terbium hydride on the surface of magnets will favor the increase in the oxygen content in magnets. According to differential thermal analysis (DTA+TG) data (heating in an argon atmosphere (Ar 6N) at a rate of $10^\circ\text{C}/\text{min}$, the dysprosium hydride (DyH_2) decomposition takes place at 930°C (figure 3b).

2.3. Study of magnetic characteristics of $Nd_2Fe_{14}B$ magnets prepared with REM hydrides

The initial alloy in the form of flakes 300 μm in thickness was prepared by “strip-casting” technique [5]. The chemical composition (wt %) of the alloy is Nd-24.0, Pr-6.5, Dy-0.5, B-1.0, Al-0.2, Fe-balance. Flakes were subjected to hydrogen decrepitation in dry-hydrogen flowing atmosphere at 100°C for 1 h and subsequently passivated in gaseous nitrogen. After cooling the powder to room temperature, terbium hydride (2 and 4 wt %) or dysprosium hydride (2 wt %) were added. A mixture was subjected to fine milling for 40 min to an average particle size of 3 μm using a vibratory mill and isopropyl alcohol medium. After compaction in a magnetic field and sintering at 1070°C (for 2 h), the sintered blanks prepared with the terbium hydride were subjected to heat treatment (HT) 900°C (2 h) + 530°C (1 h) + 500°C (1h). The optimum heat treatment for magnets prepared with the dysprosium hydride is 1-h annealing at 500°C (HT1). The stability of hysteretic properties of the magnets prepared with DyH_2 was tested using heat treatments (HTs): HT-2 (500°C (1 h) + quenching + 500°C (2h) + cooling for 2 h to 400°C + 400°C (6 h) + furnace cooling); HT-3 (500°C (1 h) + quenching + 500°C (2h) + cooling for 2 h to 400°C + 400°C (6 h) + furnace cooling + 550°C (1h) + quenching); HT-4 (HT-1 + HT-2 + HT-3 + 1050°C + 500°C (2 h) + quenching in gaseous nitrogen).

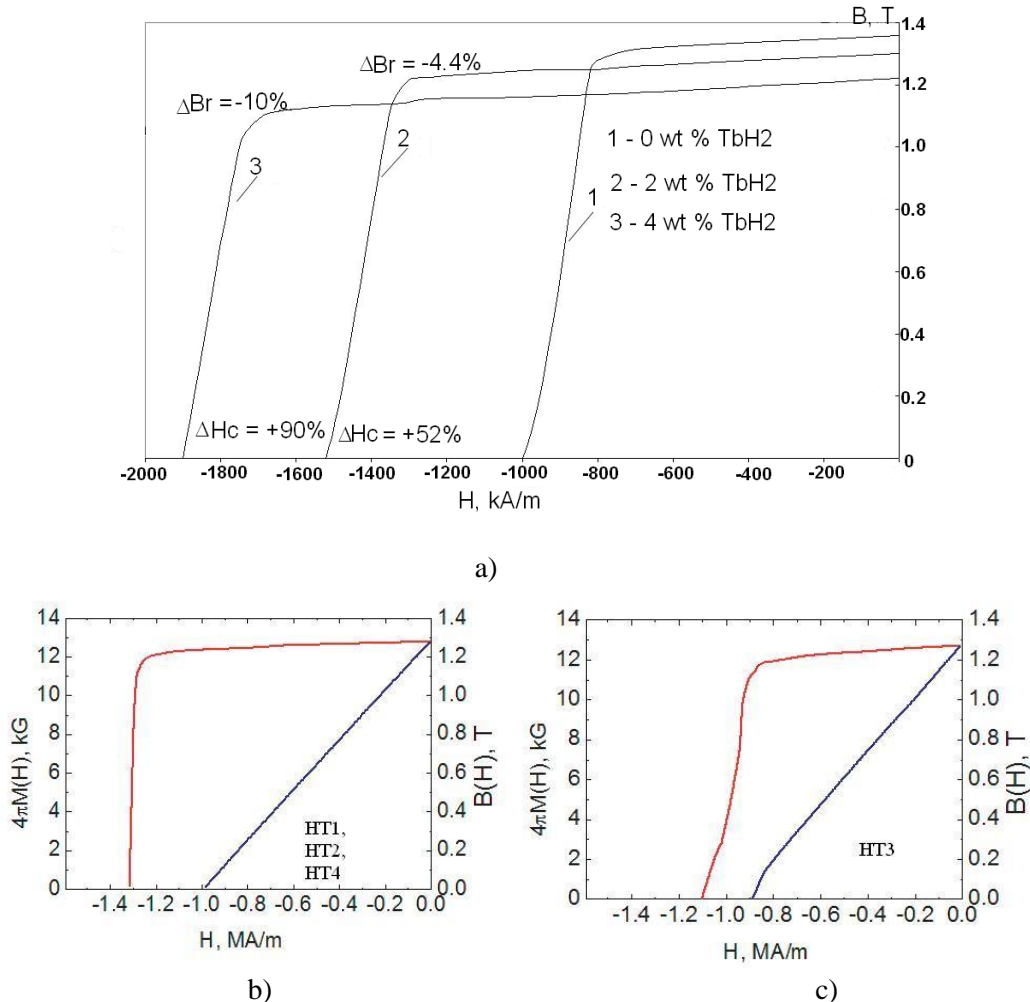


Figure 4. Magnetization reversal portions of hysteresis loops for the Nd-Fe-B sintered magnets prepared with (a) 0, 2, 4 wt % TbH₂ and (b,c) 2 wt % DyH₂ after (b) optimum (HT1), stepped (HT2), restoring (HT4) and (c) degrading (HT4) heat treatments.

Magnetic characteristics of samples were measured after grinding and saturation magnetization.

The measurements were performed at room temperature in magnetic fields up to 3 T using a close circuit of hysteresimeter. Figures 4a, b, c demonstrates the variations in the hysteresis loop, which are caused by the application of hydride additions and heat treatments.

For all samples, curves of magnetization from the thermally demagnetized state and dependences of jH_c и B_r on the magnetized field are typical of magnets whose magnetization reversal mechanism is due to the delayed nucleation of reversed domains. The magnetic parameters correspond to permanent magnets prepared in the oriented magnetic field (1200 kA/m) perpendicular to pressing direction.

When applying the terbium hydride for the Nd-depleted Nd-Fe-B-based compositions, we found some peculiarities of REM distribution within the magnet structure [17]. The formation of the high-coercivity state of the Nd-Pr-Dy-Fe-B sintered magnets prepared by blending technology in applying TbH_2 in the powder mixture is discussed from the point of view of nonuniform distribution of REMs within 2-14-1 phase grains. This effect manifests itself more substantially with increasing contents of alloying elements (in total case, heavy rare-earth metals) and in using some manufacturing processes, (“strip casting”, mechanical alloying, hydrogen decrepitation, etc.). The nonuniformity of principal hard-magnetic phase leads to the increases in structurally sensitive magnetic parameters, such as H_k , B_r , jH_c . Moreover, the data obtained for magnets with DyH_2 addition demonstrate the higher thermal stability of hysteretic properties. The observed effect also is attributed to the formation of nonuniform Dy distribution in $(Nd, Pr, Dy)_2Fe_{14}B$ principal magnetic phase grains, which is formed during the preparation of material from hydride-containing powder mixtures and determines the specificity of diffusion processes occurred during low-temperature annealing; the effect also is discussed in terms of continuity and discontinuity of grain boundaries [18]. These data are of importance for deciding the optimum heat treatment of Nd-Fe-B magnets and prediction of their service stability.

3. Conclusions

Possibilities of distillation purification of REMs and peculiarities of the structure of distilled metals are discussed. Hydrides TbH_2 and DyH_2 were synthesized and used as efficient additions to powder mixtures for manufacturing sintered Nd-Fe-B permanent magnets. The hysteretic characteristics of the magnets were reached in using the initial Nd-depleted strip-casting alloy and economical alloying with heavy REMs (Dy, Tb). The results obtained allow us to conclude that the suggested modification of the manufacturing process of sintered magnets (the use of REMs’ hydrides) corresponds to the modern world tendency in their production, which consists in the saving of deficient expensive REMs. Moreover, the modified variant of the manufacturing process allows us to prepare magnets with the wide range of hysteretic characteristics in using a unified initial Nd-Fe-B alloy.

Acknowledgments

This study was supported by the ERA_NET_RUS_PLUS, project no. INNO_146, Russian Academy of Sciences (program no. IV.5.6) and project No. LO1203 (Czech Republic).

References

- [1] Gschneidner K A Jr. 1989 *Proceeding of the 1st Rare Metals Forum* (Tokyo, Japan: Society of Non-Traditional Technology) 13
- [2] Glebov V A and Lukin A A 2007 *Nanocrystalline Rare-Earth Hard Magnetic Materials* (Moscow: Publishing House “FGUP VNIINM”), in Russian
- [3] Li W F, Sepehri-Amin H, Ohkubo T and Hono K 2011 *Acta Materialia* **59** 3061
- [4] Sepehri-Amin H, Ohkubo T and Hono K 2010 *J. Appl. Phys.* **107** 745
- [5] Glebov V A, et al 2011 *Fiz. Chim. Obrab. Mater.* 3 16
- [6] Watanabe N, Umamoto H, Ishima M, Itakura M, Nishida M, and Machida K 2009 *J. Microscopy* **236** (2) 104
- [7] Sepehri-Amin H, Ohkubo T and Hono K 2013 *Acta Materialia* **61** 1982
- [8] Kianyashi A, Mottram R S and Harris I R 1999 *J. Alloys Comp.* **287** 206
- [9] Wang H, Li A and Li W 2007 *Rare Met. Mater. Eng.* **36**(6) 1088

- [10] Gaolin Y, McGuinness P J, Farr J P G and Harris I R 2010 *J. Alloys Comp.* **491** L20
- [11] Kim T-H, Lee S-R L, Kim H-J, Lee M-W and Jang T-S 2014 *J. Appl. Phys.* **115** 17A763
- [12] Liu W Q, Li C, Zakotnik M, Yue M, Zhang D T and Zuo T Y 2014 *Proceeding REPM2014* (Annapolis, Maryland, USA) 116
- [13] Yartys V A, Gutfleish O, Panasyk V V and Harris I R, 1996 *J. Alloys Comp.* **253** 128
- [14] Gabis I, Evard E, Voyt A, Chernov I and Zaika Yu 2003 *J. Alloys Comp.* **356/357** 353
- [15] Devyatykh G G and Burkhanov G S 1997 *High-Purity Refractory and Rare-Earth Metals* (Cambridge: Int. Sci. Publ.)
- [16] Burkhanov G S, Kolchugina N B, Tereshina E A, Tereshina I S, Politova G A, Chzhan V B, Badurski D, Chistyakov O D, Paukov M, Drulis H and Havela L, 2014 *Appl. Phys. Lett.* **104** 242402
- [17] Lukin A A, Kolchugina N B, Burkhanov G S, Klueva N E and Skotnicová K 2013 *Inorg. Mater.: Appl. Res.* **4** 256
- [18] Burkhanov G S, Lukin A A, Kolchugina N B, Koshkid'ko Yu S, Dormidontov A G, Skotnicová K, Zivotsky O, Čegan T and Sitnov V V 2014 *Proceedings REPM2014* (Annapolis, Maryland, USA)